Deuteron-Proton Scattering Using Photographic Techniques* †

F. A. Rodgers,‡ H. A. Leiter,¶ and P. G. Kruger
Physics Department, University of Illinois, Urbana, Illinois
(Received November 7, 1949)

The differential scattering cross section for 9.94±0.08-Mev deuterons scattered by protons has been determined with nuclear track emulsions as detectors. The deuterons were obtained from the cyclotron while the target consisted of hydrogen gas at a pressure of approximately 5 cm of mercury.

The photographic plates were arranged so that they recorded simultaneously at all laboratory angles from 12.5° to 65°. Approximately 5000 proton tracks at each of 12 angles in this range were counted. Geometrical, slit scattering, and slit penetration corrections have been made to the number of tracks counted.

I. INTRODUCTION

Experiments on the scattering of protons by deuterons have been reported by Tuve, Heydenburg, and Hafstad[1] in which the incident protons had energies up to 830 kev and by Taschek[2] at much lower energies. Primakoff[3] and Ochial[4] have attempted a theoretical analysis of the results obtained by Tuve, Heydenburg, and Hafstad. Their conclusions were that the experimental work showed anomalies which they could not explain. Sherr, Blair, Kratz, Bailey, and Taschek[5] have recently reported results in the energy range from 0.825 to 3.49 Mev which show a rather uniform decrease in cross section with increasing energy. Furthermore, their results in the neighborhood of 830 kev did not show the anomalies obtained by Tuve, Heydenburg, and Hafstad.

All the workers mentioned above used electrical detection methods and scattered protons by deuterons, probably because of the simplification this afforded in the analysis of the data. In the present work photographic detection methods were used to measure the scattering of deuterons by protons. This choice of bombarding particle was made for convenience in analysis.

The use of photographic plates in scattering experiments has several very definite advantages over other common methods of detection. The plates are continuously sensitive in contrast to the small sensitive time of cloud chambers. They also can be used to register simultaneously over a large range of scattering angles while maintaining angular definition. This is in sharp contrast to the restrictions on electrical detection methods. Finally, the extreme simplicity of the photographic plate as a detection unit would alone be a strong point in its favor.

The main disadvantage associated with photographic plates arises in the analysis of the data. The analysis can be very tedious in those uses where different nuclei have to be distinguished, the energy has to be determined, or the angle has to be measured for each particle. However, the present experiment was arranged so that none of the above information had to be determined from measurements on the track. Instead, all that was required was a determination of the number of proton tracks registered at a given angle.

Chadwick, May, Pickavance, and Powell[6] reported preliminary results from a chamber designed for scattering of light nuclei from a gas target which used one plate to record all data from 10° to 170° in the laboratory system. They gave an excellent summary of the advantages derived from photographic plates and of the problems peculiar to their use. More recently, Dearnley, Oxley, and Perry[7] have used photographic plates to determine the absolute cross section for proton-proton scattering in which they used rectangular defining slits and registered data from 10° to 45° in the laboratory system.

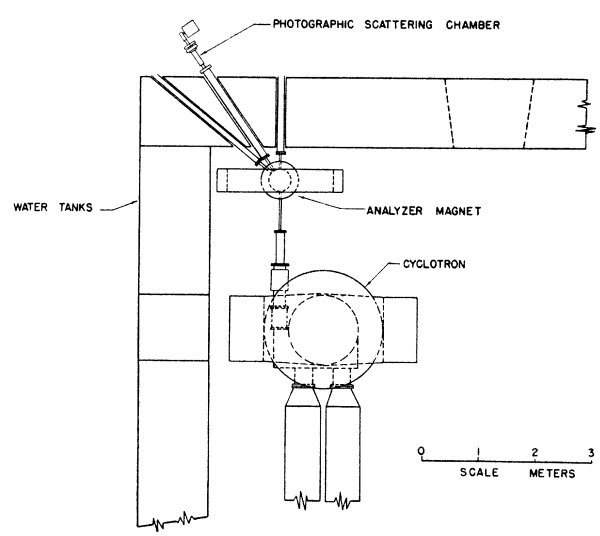

Fig. 1. Plan view of cyclotron and scattering chamber.

* Submitted in partial fulfillment of the requirements for the Ph.D. by F. A. Rodgers.

† This work has been supported jointly by the ONR and AEC.

‡ Now at the University of Wisconsin, Madison, Wisconsin.

¶ Now with the Westinghouse Laboratories, Pittsburgh, Pennsylvania.

[1] Tuve, Heydenburg, and Hafstad, Phys. Rev. **50**, 806 (1936).
[2] R. F. Taschek, Phys. Rev. **61**, 13 (1942).
[3] H. Primakoff, Phys. Rev. **52**, 1000 (1937).
[4] K. Ochial, Phys. Rev. **52**, 1221 (1937).
[5] Sherr, Blair, Kratz, Bailey, and Taschek, Phys. Rev. **72**, 662 (1947).
[6] Chadwick, May, Pickavance, and Powell, Proc. Roy. Soc. **183**, 1 (1944).
[7] Dearnley, Oxley, and Perry, Phys. Rev. **73**, 1290 (1948).

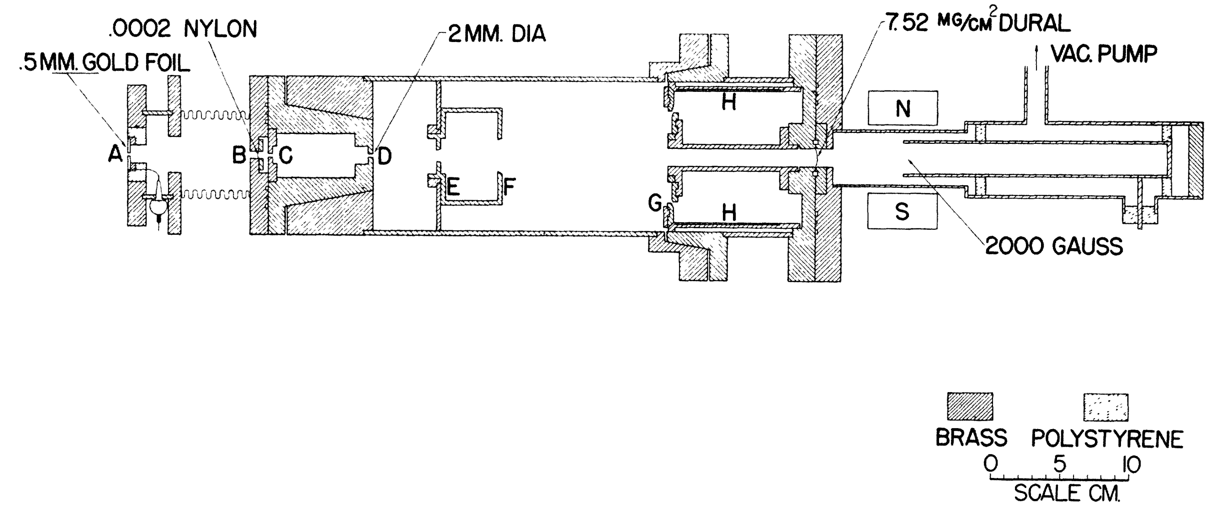

FIG. 2. Cross section of the scattering chamber and Faraday cage. A. Gold foil slit for stopping down the deuteron beam. B. Nylon foil separating cyclotron vacuum from scattering chamber. C, D. Two-mm collimating slits. E, F. Antiscattering baffles. G. Annular slit. H. Photographic plate tangent to inside circumference of cylinder.

II. SCATTERING APPARATUS

The scattering chamber was located in front of the 37° exit tube of the University of Illinois cyclotron as shown in Fig. 1. The deuteron beam from the cyclotron passed down the exit tube, through the magnetic analyser, and out the exit tube which passes through the water tanks surrounding the cyclotron. Figure 2 shows the details of the scattering chamber. The deuteron beam was stopped down to a diameter of 4 mm by a gold foil located 4 in. in front of the first collimating slit of the scattering chamber. The gold foil was insulated so that the current to it could be registered and this current served as a monitor during the experimental runs.

The two collimating slits (C and D) were each 2 mm in diameter and spaced 3 in. apart. They were carried in a ground brass cone to facilitate removal and also to guarantee exact positioning upon replacement. The divergence of the beam after collimation was found by placing a photographic plate at the back of the scattering chamber and allowing the beam to strike it for an instant. This method gave a half-angle divergence of approximately 11 min. The small value is largely due to the distance between the cyclotron and the scattering chamber. It was increased to approximately 17 min. by the presence of hydrogen at a pressure of approximately 5 cm of mercury in the scattering chamber and a 0.2-mil Nylon foil $\frac{1}{4}$ in. in front of the first collimating slit which separated the hydrogen gas in the scattering chamber from the high vacuum of the cyclotron and exit tube.

The detection of the scattered particles occurred in the "camera" which held an annular defining slit and the photographic plate holder. All but 120° of the annular slit was open so that six photographic plates could be exposed at the same time, thus using about 180° of the azimuthal angle. The annular slit and camera were so designed that all laboratory scattering angles from 12.5° to 65° could be recorded simultaneously. In order to obtain this advantage the slits had to be designed so that some particles could penetrate through the edges of the slit. This effect will be considered later.

The camera, like the collimating slit holder, was sealed on to the scattering chamber by means of a ground brass cone. A black cloth covered the camera and flange when the camera was removed to the dark room. The undeflected particles passed down the inner tube of the camera, through the 7.5-mg/cm² aluminum foil at the back of the camera, and into the Faraday cage.

The six photographic plates were supported on a brass cylinder so that the plane of the emulsion and the long edge of the plate were parallel to the unscattered deuteron beam. Three-by-one-inch Ilford nuclear track plates, Type C-2, with an emulsion thickness of 50μ were used. The position of a track on the plate and the position of the plate relative to the annular slit determined the angle of scattering, eliminating the necessity of measuring the angle of each track.

To prevent any deuterons which might scatter off the last collimating slit from reaching the photographic plate, antiscattering baffles were included (see Fig. 2). These were designed so that the last collimating slit could see neither the annular slit nor the walls of the chamber beyond the antiscattering baffles.

III. AUXILIARY APPARATUS

The undeflected deuterons were collected in a Faraday cage and the charge collected, integrated by a low current Q-meter. This apparatus as well as the method of calibrating the Q-meter is described elsewhere.[8] An error of one percent has been ascribed to the value of the resistance and an error of one percent to calibration voltage. This gives a value of 1.4 percent error[9] in the charge measurement.

The scattering chamber was evacuated by means of a 10-liter per sec. oil diffusion pump backed by a mechanical fore pump. Without photographic plates in the chamber the pressure could be reduced to about 7×10^{-6} mm of mercury as measured by an ionization gauge. With plates in the camera the pressure could be reduced to less than 5×10^{-5} mm of mercury after 24 hr. After closing off the scattering chamber from the pumps a rate of rise occurred of about 1.5×10^{-4} mm of mercury per min.

The hydrogen was admitted to the system through a heated palladium tube. Both the palladium tube and the diffusion pump were separated from the scattering chamber by liquid air traps to reduce the chance of contamination. The pressure of the hydrogen in the chamber was measured by means of an oil manometer, the difference in height being measured by a cathetometer. The oil manometer was constructed of $\frac{1}{2}$-in. inside diameter glass tubing and filled with Octoil-*S*. The density of Octoil-*S*, which has been outgassed, has been measured[10] to be

$$0.9104[1-0.000733(t-25)]\ \text{g/cm}^3\pm0.05\ \text{percent},$$

where t is the temperature of the oil in degrees centigrade. This is in good agreement with the manufacturer's value of 0.9103 g/cm³. The vapor pressure of Octoil-*S* has been given by the manufacturer as 7×10^{-9} mm of mercury. The "closed" side of the manometer was pumped continuously by the oil diffusion pump associated with the scattering chamber. The temperature was measured by a thermometer placed with the bulb inside the chamber near the scattering volume and the stem outside the chamber.

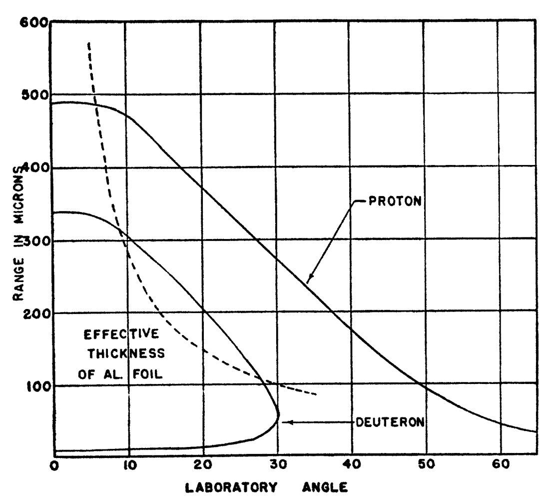

FIG. 3. Range of recoil protons and scattered deuterons in Ilford C-2 emulsion. The differences between the dashed line and the solid lines give the residual range of the particles in the emulsion when 19 mg/cm² aluminum foil is placed over the emulsion.

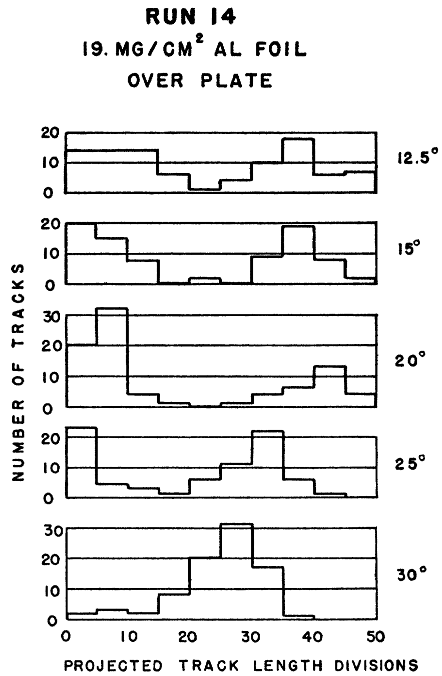

FIG. 4. Histograms of track lengths as seen projected on the eyepiece scale of the microscope.

The photographic plates were studied under a binocular microscope using bright field illumination and a magnification of about 260 times. The plates were held in a plate holder designed so that the means of positioning the plates were the same as in the camera plate holder. This was necessary since the edges of the photographic plate were not even and thus the edges of the plate holder had to serve as reference lines.

IV. EXPERIMENTAL PROCEDURE

A preliminary consideration of deuteron-proton scattering based on conservation of energy and momentum showed that the range of the scattered and recoil particles in the emulsion, as a function of laboratory angle, is as shown in Fig. 3. This shows that above 30° only proton recoils occur while below 30° three groups of particles occur—(1) recoil protons, (2) low energy scattered deuterons corresponding to large scattering angles in the center-of-mass system, and (3) high energy scattered deuterons corresponding to small scattering angles in the center-of-mass system.

All three low angle groups could be allowed to register on the photographic plate, but in this case even if 100μ-thick emulsions were used the distinction between proton and deuteron tracks would require a careful examination of each of the tracks.

By a fortunate combination of geometry and the range relation shown in Fig. 3, it was possible to place

[8] R. E. Meagher, Phys. Rev. **78**, 667 (1950).
[9] See footnote 13 of reference 8.
[10] Measured by E. J. Zimmerman.

a 19.0-mg/cm^2 aluminum foil over that part of the plate which registered deuterons, reducing the length of the registered tracks to a point where the differentiation between proton and deuteron tracks was easy. This was due to the fact that the deuteron tracks were only about 25 percent as long as the proton tracks when the 19.0-mg/cm^3 foil was in place rather than 80 percent as long. Another advantage in using the aluminum foil was that a smaller fraction of the particles which penetrated the slit edge were allowed to register on the plate at those angles at which the penetration factor otherwise would have been the largest.

The effect of the aluminum foil is shown by histograms, given in Fig. 4, of the track lengths observed at various angles. The scattering in the aluminum foil and the emulsion broaden the peak somewhat, but the proton group remains well defined.

An experimental run was started by loading the camera and placing the camera, Faraday cage, and Q-meter in position. The systems were allowed to pump down for approximately 24 hr., the last 6 hr. with liquid air on the traps, in order to get rid of the water vapor from the photographic plates. After the pressure had dropped below 5×10^{-5} mm of mercury in the scattering chamber, the Q-meter was calibrated. The scattering chamber was then closed off and filled with hydrogen. After filling, the system was allowed to stand for 10 min. to come to equilibrium and then the pressure and temperature of the hydrogen were read. The plates were then exposed by passing a deuteron beam of about 10^{-9} amp. through the scattering chamber for about one-half hour. This was sufficient to give approximately 2500 tracks at each experimental point. After the exposure, the pressure and temperature of the hydrogen were re-measured and the Q-meter re-calibrated. The hydrogen pressure increased about 0.2 percent during the run do to the change in liquid air level in the traps. This change was linear with time and therefore the average pressure during the run was used in the calculations.

The camera was then removed to the dark room and the photographic plates were developed for 15 min. in Kodak D-19, diluted four to one, and fixed for 45 min.

In addition to two runs as described, a vacuum scattering run was made to determine the effectiveness of

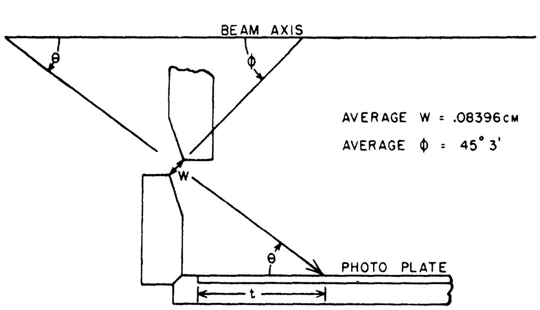

FIG. 5. Geometry for the distance, t, along the photographic plate corresponding to a scattering angle, θ.

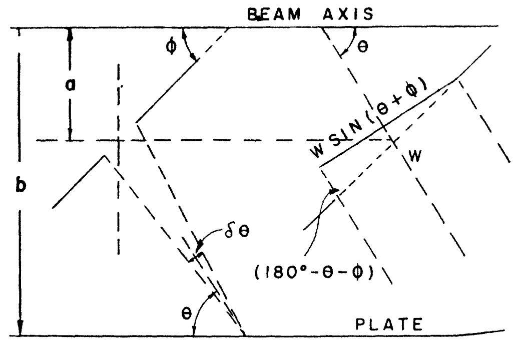

$$\delta\theta = \frac{W\ \sin(\theta+\phi)\ \sin\theta}{(b-a)}$$

FIG. 6. Geometry for calculating $\delta\theta$. $\delta\theta$ is defined as the angle subtended by the annular slit at the swath on the photographic plate.

the scattering baffles. This run was similar in every way to the regular run except that after closing off the scattering chamber from the pumps a time equal to that required to fill with hydrogen was allowed to elapse before the beam was turned on.

V. CONSTANTS OF THE APPARATUS

The laboratory cross section is given as a function of the laboratory angle, θ, by

$$\sigma_{\mathrm{lab}}(\theta)=N(\theta)/n_in_t\mathfrak{L}(\theta)\delta\Omega, \tag{1}$$

where $N(\theta)$ = number of proton tracks counted, n_i = number of incident deuterons, n_t = number of target hydrogen atoms per cm^3, $\mathfrak{L}(\theta)$ = beam length effective at the angle θ, and $\delta\Omega$ = solid angle recorded at the angle θ.

The geometrics from which θ and $\delta\theta$ were determined are shown in Figs. 5 and 6, respectively. Since a given swath on the photographic plate records over an angle increment, $\delta\theta$, equal to the polar angle subtended by the annular slit at that swath, this angle, $\delta\theta$, is the polar angle contribution to the expression for $\delta\Omega$.

At each angle in this interval,

$$(\theta_0-\delta\theta/2)<\theta<(\theta_0+\delta\theta/2);$$

the effective length of the beam is just equal to the swath width since the photographic plate is parallel to the beam. This effective length is obtained by extending a line from each side of the swath inclined at an angle, θ, to the beam until they intersect the beam. In some cases more than one swath was used in order to obtain a sufficient number of tracks. In these cases the swaths were taken immediately adjacent to each other. Thus in these cases

$$\mathfrak{L}(\theta)=S\cdot w, \tag{2}$$

where S is the number of swaths per plate and w is the swath width.

The quantities which are functions of the angle are

TABLE I. Constants of the experiment.

Swath width, $w=0.01869\pm0.00005$ cm
Slit width, $W=0.08396\pm0.00008$ cm
Slit angle, $\phi=45°\ 3'\pm12'$
Plate radius, $b=4.780\pm0.005$ cm
Slit radius, $a=3.173\pm0.002$ cm
Axial distance from slit to swath $=(t+0.2396)\pm0.004$ cm
Swath length, $h=1.000\pm0.004$ cm, or
$=1.500\pm0.004$ cm
Energy of deuterons $=9.94\pm0.08$ Mev
Acc. due to gravity, $g=980.139$ cm/sec.[2]

given as

$$\theta=\tan^{-1}(b-a)/(t+0.2396\text{ cm}), \tag{3}$$

$$\delta\theta=W\sin(\theta+\phi)\sin\theta/(b-a), \tag{4}$$

$$\delta\beta=2\text{ (No. of plates) }\tan^{-1}\text{ (swath length/2b)}, \tag{5}$$

and since there are six plates,

$$\delta\beta=12\tan^{-1}(h/2b), \tag{6}$$

where h = swath length. Thus

$$\sigma_{\text{lab}}(\theta)=(b-a)N(\theta)/n_in_tSwW\sin(\theta+\phi)\sin^2\theta\delta\beta.$$

The conversion to the center-of-mass cross section is given by

$$\sigma_{\text{C.M.}}(\alpha)=\sigma_{\text{lab}}(\theta)d\Omega_\theta/d\Omega_\alpha. \tag{7}$$

The scattering angle in the center-of-mass system will be defined in the present work as the angle through which the particles are deflected. With this convention there is no ambiguity concerning which particle is the incident particle in the laboratory system.

By use of this convention the relation between the recoil angle, θ, of the proton in the laboratory system and the corresponding center-of-mass angle, α, is given by

$$\alpha=(180°-2\theta), \tag{8}$$

while

$$d\Omega_\alpha/d\Omega_\theta=\sin\alpha d\alpha/\sin\theta d\theta=4\cos\theta. \tag{9}$$

Table I summarizes the measurements of the required dimensions of the apparatus.

The swath width was defined by the ends of a scale in one eyepiece of the binocular microscope as the plate passed under the objective. In counting the tracks, the point at which a particle entered the emulsion was taken as the defining position of the track. The swath width on the photographic plate, as defined by the eyepiece scale, was determined by direct measurement on an optical comparator.

W and ϕ were determined by measurements made on an optical nodal slide. This instrument was well adapted for these measurements since the slit system could be clamped in the nodal slide and then readily turned so that the axis of the slit system made any angle up to 60° with respect to the axis of the microscope. The projected openings of the slit at 45° and 60° to the axis of the slit holder were measured at 12 positions around the slit, and from these data both W and ϕ were determined from geometrical considerations.

The average deviation from the mean value of W of individual values was 0.3 percent, but any individual reading and therefore the average value of W was accurate to 0.1 percent. ϕ on the average varied by 39′ from the mean while the average was considered accurate to 12′.

The energy of the beam was determined[11] by a method involving a differential ionization chamber similar to that described by Dearnley, Oxley, and Perry[7]. This gave an energy for the deuteron beam of 10.00 ± 0.07 Mev. This had to be corrected for the 0.2-mil Nylon foil which was equivalent to 0.5 cm air or 0.04 Mev and the energy loss due to the hydrogen gas to the 45° scattering volume of 0.016 Mev. This, then, gives an energy of 9.94 ± 0.08 Mev at the center of the scattering volume. The extra 0.01 Mev in the uncertainty is to take account of the variation in energy from one scattering volume to another.

The angular definition in this experiment has two contributions. The larger contribution is given by Eq. (4). The smaller contribution is given by the angle subtended by the swath width at the annular slit. The half-angle width contributed by these two effects ran from about 1° to 2° at scattering angles of 12.5° and 55°, respectively.

Two experimental runs were made to obtain approximately a total of 5000 tracks at each angle. The data were taken in two runs in order to keep down the density of tracks for ease in counting.

The hydrogen pressure, temperature and Q-meter constants are functions of the run and are given in Table II for each of the two runs.

VI. CORRECTIONS

In order to allow simultaneous registration at many polar angles the annular slit must be designed in such

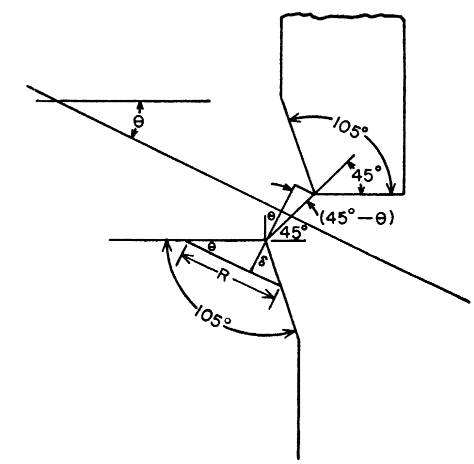

FIG. 7. Geometry for determining the penetration factor for the annular slit.

[11] Determined by C. J. Taylor.

Table II. Constants of the runs.

	Run 14	Run 16
H_2 pressure	75.00±0.02 cm of oil	75.43±0.02 cm of oil
H_2 temperature	25.7±1°C	22.8±1°C
Oil temperature	23.1±1°C	20.5±1°C
Oil density	0.9117 g/cm³±0.1%	0.9134 g/cm³±0.1%
Q-meter counts	12,160	12,161
Coulombs/count	$1.028\times10^{-10}\pm2\%$	$1.031\times10^{-10}\pm2\%$
Coulombs	$1.250\times10^{-6}\pm2\%$	$1.254\times10^{-6}\pm2\%$
n_i	$7.80\times10^{12}\pm2\%$	$7.83\times10^{12}\pm2\%$
n_t	$3.249\times10^{18}\pm0.35\%$	$3.306\times10^{18}\pm0.35\%$

a way that particles can, to a certain extent, penetrate through the edges of the slit. This results in an effective widening of the slits over the optical width. Those particles which penetrate through the edges of the slit also give shorter tracks in the emulsion than those which go through the open slit, an effect that produces a short-track tail on the track length spectrum. The fraction of the total number of tracks recorded at any angle which are due to particles which have penetrated the slit can be determined from the geometry of Fig. 7 as

$$\frac{N_p}{N_0}=\frac{2R\sin(\theta)\sin(75°-\theta)}{W\cos(45°-\theta)\sin75°}, \tag{10}$$

where N_p is the number of penetration particles, N_0 is the number of particles passing through the open slit, and R is the penetration thickness corresponding to the minimum track length accepted in the counting. R is determined by both the integral stopping power of the emulsion and the stopping power of the brass. The integral stopping power for the emulsion was determined from the length of the tracks at various angles and the known energy in the proton-proton experiment.[8] These were compared with the stopping power curves as given by Lattes, Fowler, and Cuer[12,13] for protons in Ilford emulsions with which they agreed to within five percent. The range in mg/cm² for the brass was determined using the range curves for copper given by Aron.[14] The penetration factors which have been calculated from Eq. (10) are given in Table III. The limits on the corrections are based on the probable errors in the stopping power of the Ilford emulsions and the statistics of the penetration counts.

An attempt was made to verify experimentally these calculated penetration factors without too much success. Theoretically a set of slits could be constructed in which the edges of the slits just touched. Then a run with these slits would give just the penetration tracks and the correction could be made experimentally. Actually, a set of "closed" slits of this type could not be constructed which were accurate enough to give any significant results. At some points around the annular slit, the slit would be slightly open and at other points slightly overlapping.

[12] Lattes, Fowler, and Cuer, Nature **159**, 301 (1947).
[13] Lattes, Fowler, and Cuer, Proc. Phys. Soc. London **59**, 895 (1947).
[14] *Handbook of Radioactivity and Tracer Methodology* (1948), Air Force Technical Report No. 5669, p. 183.

TABLE III. Slit penetration correction and target length at laboratory scattering angles.

θ in degrees	$\mathcal{L}(\theta)$ in cm	N_p/N_0 in percent
12.5	4.0	1.3±0.4
15	3.0	2.5±0.5
20	3.0	3.8±0.5
25	2.0	4.6±0.7
30	1.5	5.4±0.8
35	1.5	4.2±0.7
40	1.5	6.9±0.6
45	1.0	4.9±0.5
50	1.0	3.4±0.3
55	1.0	2.3±0.2
60	1.0	1.2±0.1
65	1.0	0.5±0.1

The photographic plates were found to be not accurately parallel to the deuteron beam. This effect was such as to make small corrections in b, the radial distance of the plate from the beam, and in the average angle, θ. The discrepancy in b, from that given in Table I, varied linearly from -0.019 cm at the high angle end of the plate to $+0.015$ cm at the low angle end of the plate. This correction amounted to 0.35 percent in the worst case.

Another correction on b occurs because of the use of straight swaths on the photographic plate. The intersection of the plane of the photographic plate with the cone of constant polar scattering angle is a parabola. Thus the swath should be parabolic rather than straight. The average value of b along a given swath is greater than the value at the center of the swath by one-third

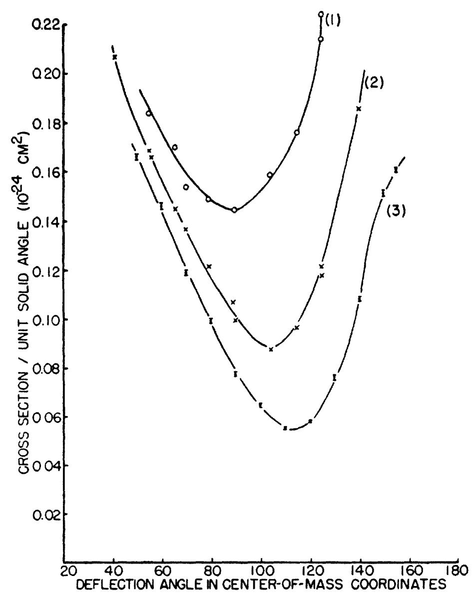

FIG. 8. Deuteron-proton center-of-mass differential cross sections. (1) 1.5-Mev protons incident on deuterium. Sherr *et al.* (2) 3.0-Mev protons incident on deuterium. Sherr *et al.* (3) 9.94-Mev deuterons incident on hydrogen. Present data.

TABLE IV. Scattering cross sections.

No. counts	θ_{lab}	$\sigma_{lab}\times10^{24}$ cm^2	$\theta_{C.M.}$	$\sigma_{C.M.}\times10^{24}$ cm^2	$(N)^{\frac{1}{2}}/N$
5620	12.5°	0.603	155	0.1543	1.3 percent
6426	15	0.577	150	0.1494	1.3
8271	20	0.404	140	0.1075	1.1
6000	25	0.274	130	0.0757	1.3
4679	30	0.197	120	0.0569	1.5
5668	35	0.178	110	0.0545	1.3
8058	40	0.195	100	0.0635	1.1
7098	45	0.216	90	0.0763	1.2
9524	50	0.251	80	0.0978	1.0
5599	55	0.267	70	0.1165	1.3
6458	60	0.284	60	0.1422	1.2
6568	65	0.273	50	0.1614	1.2

the difference in the value of b between the center and the end of the swath since the difference is proportional to the square of the distance from the center of the swath. This correction amounted to 1.22 percent in the worst case.

Finally, a correction is provided by the vacuum run. This will include the effects of slit scattering, contamination scattering and proton recoils from neutron background. The majority of the proton recoils were eliminated from the counting by visual inspection since most of them started in the body of the emulsion and not at the surface. The same criteria employed on the gas scattering runs were used in counting the tracks on the vacuum run. The vacuum background was largest at 30° where it was 0.4 percent. The majority of this must be due to recoil protons which started either in the surface or so near it that the difference could not be detected. The reason for believing this is that in the case of proton-proton scattering with this apparatus where both contamination scattering and slit scattering should be worse, the vacuum run background is negligible at all but the smallest angles.

The corrections mentioned resulted in a net correction of about seven percent at 40° where the net correction was largest.

VII. EXPERIMENTAL RESULTS

Two experimental runs were made in order to simplify the counting and to provide a method of checking for gross errors.

The results are tabulated in Table IV and plotted in Fig. 8. Run 16 was not counted above 50° since over 5000 tracks were obtained at each of these angles on run 14. All cross sections presented have been corrected as described in the previous section.

The percentage errors given with the cross sections in Table IV are those associated with statistics while the errors due to other sources are given below. The individual contributions to the errors are given with the measured quantities in Tables I–III. In addition to these there is the human error in counting. The counting was done by three observers, and it was found after an initial practice period that the three observers agreed within 0.5 percent on the proton-proton scattering experiment.[8] Because of increased difficulty in counting the deuteron-proton data, the estimated error due to this source has been increased to one percent.

Charge measurement, 1.4 percent. Human factor, 1.0 percent. $(b-a)$, 0.4 percent. Swath length, 0.4 percent. Swath width, 0.3 percent. H_2 temperature, 0.3 percent. Oil density, 0.1 percent. Slit width, 0.1 percent. Slit angle, ϕ, 0.1 percent. Penetration factor, 0.8 percent. Position on the plate, t, 0.4 percent.

The last three errors vary with angle. The values given are the largest and occur at 12.5°, 30°, and 40°, respectively. If we assume these largest errors in the last three above values and 1.3 percent average error for the statistical errors in σ (Table IV) we find the average net probable error for $\sigma_{C.M.}$ is 1.7 percent. This probable error would apply to the relative value of $\sigma_{C.M.}$ and to the absolute values except for footnote 9. If we take this into consideration, more probable values for the cross sections in Table IV would be obtained by increasing those given by 1.3 percent.

A statistical analysis of the data from Run 14 in which comparisons were made between the six photographic plates showed that in 35 percent of the cases the number of counts at a given angle varied by more than $\sqrt{N}$ from the average at that angle. A similar analysis for Run 16 gave 21 percent.

VIII. ACKNOWLEDGMENT

The authors wish to express their thanks to Professor R. E. Meagher for his cooperation throughout the experiment and help in making many of the measurements and to Professor G. F. Tape for the many helpful discussions of the problems associated with this experiment.